

CHAPTER SEVENTY THREE

INTERACTION OF NON-UNIFORM CURRENTS AND SURFACE WAVES

By Nabil M. Ismail, A. M. ASCE*

ABSTRACT

Modifications of surface gravity waves and opposing nonuniform currents due to their interaction in coastal waters were experimentally and theoretically investigated. The flow field is modelled as a steady turbulent jet heads directly into the surface waves. Experimental results show that the net waves momentum flux is decreased as waves propagate into the jet which gives rise to mean water set-up towards the jet source. Opposing waves increase the spreading rate of the jet and causes vertical upwelling of the mean flow, near the bottom, towards the free surface. Theoretical predictions of the increase of the jet spreading rate and wave set-up agree with the experimental data. Wave-current interaction modifies significantly waves bottom flow pattern by focusing ambient nearshore waters on the jet outlet.

INTRODUCTION

Over a large portion of the world's oceans and seas, the spatial distribution of surface currents generated by winds, tides and ocean circulation is so great that an understanding of wave propagation on currents is very important. An example of these nearshore ocean processes is the interaction of surface waves, propagating towards the coast, with tidal flows out of bays, river flows, and cooling water discharges from power plants. Currents in coastal waters influence wave propagation significantly due to the strong current shear and in turn the waves modify the current. These wave and current modifications play an integral role in defining the near shore dynamic characteristics. In addition, the modifications have important implications in regard to prediction of coastal sediment transport, and mixing of materials dispersed into the surf zone. Furthermore, knowledge of changes of mean water level due to wave-current interaction is necessary for numerous engineering endeavors.

The present study is directly related to the interaction of waves coming from offshore and tidal flows out of bays. There has been very limited experimental work reported in the literature on the interaction of non-uniform currents with surface gravity waves which necessitates performing of a detailed experimental study on the subject.

*Sr. Engr., Pipeline & Production Technology Division, Bechtel Petroleum, Inc., San Francisco, Calif.

The main purpose of this study is to explore experimentally and theoretically modifications of waves and non-uniform currents due to their interaction in coastal waters. The experiments were carried out for the more general of a steady turbulent jet heads directly into the surface waves. Experiments were limited to those cases for which the wave's particle oscillatory velocities are much larger than turbulent velocity fluctuations associated with the jet flow. Experimental measurements of velocity were made primarily along the longitudinal axis of the jet. The theoretical analysis and experimental work performed in this investigation were directed towards achieving the following objectives:

- o To determine experimentally modifications of the surface gravity waves; specifically, wave amplitudes and wave oscillatory water particle velocities
- o To determine experimentally and theoretically the modifications of the non-uniform flow (jet); specifically the distribution of the mean flow velocity profile over the water column, the change in the spreading rate of the turbulent jet, and mean water level
- o To assess, using a photographic system, the modifications of the bottom flow pattern resulting from either the waves forward mass transport or the jet bottom entrainment due to the interaction of one (waves or jet) with each other (jet or waves)

THEORETICAL BACKGROUND

The effect of large-scale fluid motion on wave propagation has been the subject of a number of relatively recent studies. The dynamics of these wave trains can be expressed in terms of the "wave action conservation principle" established by Bretherton and Garrett (2). It is given by

$$\frac{\partial}{\partial t} \left(\frac{E}{\omega_r} \right) + \nabla \cdot [(\vec{U} + \vec{C}_g) \frac{E}{\omega_r}] = 0 \quad \dots(1)$$

where \vec{U} is the nonuniform current velocity, \vec{C}_g is the vector wave group velocity, E is the wave energy density, and ω_r is the waves intrinsic frequency.

Longuet-Higgins and Stewart (10) investigated two special cases of the general case considered by Bretherton and Garrett (2) using a perturbation expansion form for the solution. The first case is when the nonuniform current velocity \vec{U} in the direction of wave propagation and the horizontal variation of \vec{U} is compensated for by vertical upwelling from below. The second case is when the horizontal variation in \vec{U} is compensated for by a small horizontal inflow from the sides. The results of their work were a crucial advance in the theory of wave-current interaction.

Among the theoretical approaches followed is one which is a direct integration of the equations of motion with respect to the water depth and averaging over the phase of the fluctuating motion [Phillips (11)].

Crapper (3) considered the interaction of nonlinear deep water gravity waves and a steady nonuniform current, using the average Lagrangian method due to Whitham (12). His theoretical results showed that the rate of amplification of large waves is less than that of the essentially linear theory of Longuet-Higgins and Stewart (10).

Determining the back interaction of the wave field on the current mean flow is fraught with little difficulties. Hasselmann (5) and Garrett (4) emphasized that Phillips' approach yields the force exerted by the waves on the complete flow, consisting of the mean flow plus the wave field. Part of this force causes a change in the wave momentum rather than the momentum of the mean flow. Therefore, the rate of change of the wave momentum should be subtracted from the total force, in order to obtain the net force exerted by the waves on only the current flow. However for the purpose of analysis of the experimental results obtained in this study, a momentum balance of the complete flow is appropriate for the theoretical representation of the flow field.

Parameters Scaling

For the case of surface gravity waves propagating on a steady nonuniform flow, it is natural to consider the ratios of the independent parameters of the waves to those of the turbulent jet. Take L , b the longitudinal and transverse distances, and U_* , the longitudinal surface velocity at $y = b$, as the characteristic lengths and velocity scales of the turbulent jet (Fig. 1). Take L , the wave length, and C , the wave phase speed as the characteristic length and velocity scales of the waves. These scales lead to non-dimensional group [Ismail (6)]

$$G = \frac{b}{L} \frac{L \sqrt{g\pi/L}}{U_*} = \frac{b}{L} \frac{C}{U_*} = \frac{r}{L} \quad \dots(2)$$

This group corresponds to the ratio of the radius of curvature, r , of the wave rays due to the refraction by the vorticity of the horizontal shear flow ξ , to the incident wave length L . The ranges of wave and current independent variables employed in the experiments were selected in a manner to keep the value of the parameter G larger than one. This restriction was done to focus on the direct dynamical aspects of interaction between the waves and the current.

Taking α as number characterizing the ratio of the wave velocity fluctuation \tilde{u}_* to the jet characteristic surface mean velocity U_*

$$\tilde{u}_* = \alpha U_* \quad \dots(3)$$

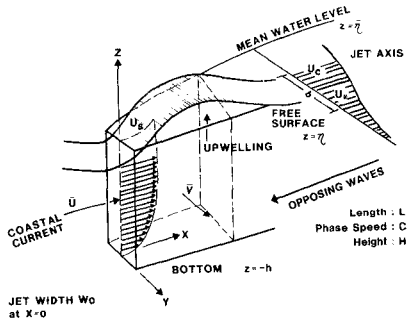


FIG. 1 Definition Sketch

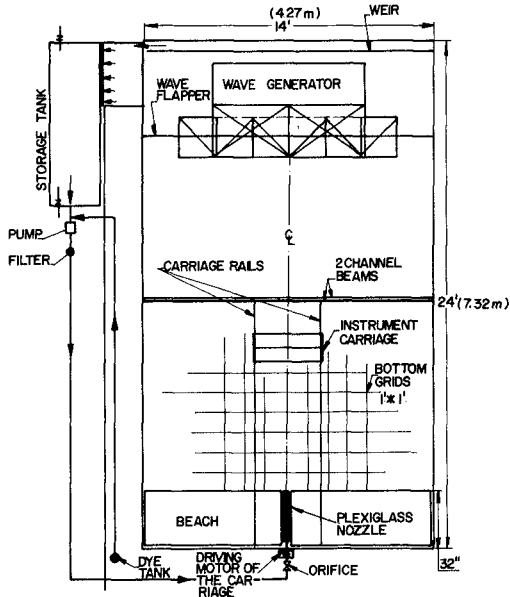


FIG. 2 Plan View of the Experimental Arrangements

For the case of waves propagating on currents in coastal waters, α is roughly of the order 0.5-1.0.

Taking β as a number characterizing the ratio of the velocity scales of the turbulent fluctuations and the time mean longitudinal surface velocities can be written as

$$u'_* = (\overline{u'_i u'_i})^{1/2} = \beta U_* \quad \dots(4)$$

in which U_* is defined as U at $y = b$. On a spatial average, β is roughly of the order of 0.25.

Taking ϵ as a number characterizing the relative water depth kh where k is the surface wave number and h is the water depth. Wave and current parameters are assumed to be uniformly distributed over the water depth for the range of the parameter $\epsilon \approx 0.5-1.0$ considered in this analysis.

Momentum Balance of the Wave Current Flow

The equation describing the momentum balance of the complete flow follows that of Phillips (11), except we will be including the bottom shear stresses into the momentum considerations. Further, we expand the time mean horizontal velocity of the complete flow \bar{u}_i into the time average of the mass flux due to the current U_i and the wave mass transport velocity U_{mi} into the momentum balance for steady or quasi-steady complete flow to yield (9).

$$\begin{aligned} \frac{\partial}{\partial x_j} \int_{-h}^{\bar{\eta}} \rho U_i U_j dz = & -\rho g(\bar{\eta} + h) \frac{\partial \bar{\eta}}{\partial x_j} - \frac{\partial}{\partial x_j} S_{ij} - \\ & \frac{\partial}{\partial x_j} \int_{-h}^{\bar{\eta}} \rho (U_i U_{mj} + U_j U_{mi}) dz - \frac{\partial}{\partial x_j} \int_{-h}^{\bar{\eta}} \rho \overline{U'_i U'_j} dz + \bar{\tau}_j^B \dots(5) \end{aligned}$$

where the subscripts i and j refer to horizontal components of parameters. The terms of the right hand side of Eq. (5) represent parameters which could exert a force by the wave on the complete flow. These forces which contribute to the divergence of the current flow momentum $\rho U_i U_j$ are respectively, the horizontal force due to the slope of the mean surface water level $\bar{\eta}$, the spatial gradients of the wave radiation stress S_{ij} , the convective momentum flux $\rho U_i U_{mj}$; $\rho U_j U_{mi}$ and the turbulent momentum flux $\rho \overline{U'_i U'_j}$. The last term, $\bar{\tau}_j^B$, represents the bottom shear stress.

Expressing each term of Eq. (5) in the scales introduced earlier one can approximate the momentum balance of the complete flow and partition it into separate mean flow and wave momentum balances. For the mean water level $\bar{\eta}$, one can argue that it is the sum of a wave

contribution $\bar{\eta}_w$ and of a jet mean flow contribution $\bar{\eta}_c$. The approximate x-components of the momentum balance are as follows.

Mean flow momentum

$$\frac{\partial}{\partial x} \rho \bar{u}^{-2} + \frac{\partial}{\partial y} \rho \bar{u} \bar{v} = -\rho g \frac{\partial \bar{\eta}_c}{\partial x} - \frac{\partial}{\partial y} \rho \bar{u} \bar{v} - \frac{\partial}{\partial y} \rho \overline{u'v'} + \frac{1}{2} \rho f \bar{u}^{-2} \quad \dots(6)$$

The above equation, which governs the mean flow momentum in the stream wise direction, appears similar to the classical x-momentum equation for nonbuoyant jets in shallow water. However, there is a distinction which is manifested by the appearance of the second term on the r.h.s. of the equation. This term, which is due to wave refraction, represents the dominant force on the longitudinal momentum of the jet mean flow.

Wave momentum flux

$$\rho g \frac{\partial \bar{\eta}_w}{\partial x} + \frac{\partial}{\partial x} \rho (\bar{u}^2 - \bar{w}^2) + \rho g \frac{\partial}{\partial x} \frac{\bar{\eta}^2}{\bar{\eta} + h} = 0 \quad \dots(7)$$

In the above equation, the force due to the slope of the free surface $\bar{\eta}_w$ would balance the difference between the two longitudinal gradients of the variance of the free surface and the isotropic waves momentum flux.

Jet spreading rate

The change of the spreading rate of the turbulent mean flow is determined by extending the scale analysis to the y-momentum equation to seek a relation between forces causing the spreading and the mean flow inertial terms (9). The increase of the spreading rate of the jet due to opposing waves is given by

$$\left(\frac{dB'}{dx}\right)_e = \frac{\frac{1}{2} \rho a_0^2 g / (C_0 - U_e) \cdot U_e}{0.122 \rho U_e^2 W_0} \quad \dots(8)$$

The numerator of the above expression can be thought of as the momentum action of the wave flow field on the jet flow, and is represented by the waves momentum density $\frac{1}{2} \rho a_0^2 g / (C_0 - U_e)$ times the convection jet flow velocity U_e . The denominator of this expression is proportional to the initial jet momentum flux (at the efflux point).

EXPERIMENTAL STUDY

The ranges of the undisturbed design parameters a_0/L_0 , h_0/L_0 , W_0/L_0 , x/W_0 , and U_e/C_0 were selected in a manner such that the secondary circulation flow of the jet and due to the waves do not cause the deflection of the jet, and the turbulent intensities are smaller than the values of the wave-induced particle velocities. According to the scale analysis performed in the last

section, and also to the pilot experiments which were carried in the wave tank the ranges of the design parameters to be used were determined. These ranges are shown in Table 1.

TABLE 1. RANGE OF WAVE-CURRENT PARAMETERS

Experimental Design	Parameter (still water)	Range
wave amplitude/wave length:	a_0/L_0	0.0025-0.02
wave length/water depth:	L_0/h_0	4-12
nozzle width/wave length:	W_0/L_0	0.10-0.03
jet efflux velocity/wave phase speed:	U_0/C_0	0.07-0.10
longitudinal distance/nozzle width:	X/W_0	0-80

Experimental Arrangements

The series of laboratory experiments which were performed in this study used an idealized model in which a steady turbulent jet heads directly into surface waves. The water depth was kept constant (0.114 m). The location and orientation of the mechanical wave generator, the beach (with a slope of 1:7) and the alignment of the discharge nozzle were the same for all of the experiments. An overall plan view of the experimental arrangement is given in Fig 2.

The turbulent jet was generated by pumping water from the reservoir through a plexiglas nozzle which had inside dimensions of 3.8 cm wide by 11.0 cm high, 76.0 cm in length. Excess water in the wave tank flowed over a sharp-crested weir upstream of the wave generator. Using this weir allowed a closed system to form for circulating the water and maintaining steady-state flow conditions. The experimental facility is located at the Hydraulic & Coastal Engineering Laboratory, University of California, Berkeley.

Data Acquisition System:

The data acquisition system can be divided into three subsystems:

a. A photographic system consisted of a camera mounted on a movable base above the longitudinal axis of the wave tank. The camera was used to take a series of color photographs of the jet, which was made visible by dye injected into the flow. It was also used to take a sequence of photographs of the bottom flow pattern in the tank. This was done using the flow-visualization technique of dropping dye crystals (potassium permanganate particles, 0.50 mm-0.59 mm) to the bottom of the tank, and photographing the resulting dye streaks.

b. Parallel wire wave gages were used in conjunction with a Sanborn (Series 150) recorder in order to measure the surface water elevations as a function of time at a specific location in the wave tank. A Sanborn Carrier Preamplifier (Model 150-1100 AS) was used to

supply the 2400 CPS/4.5 volt excitation for the gages. The full bridge was provided by an isolation transformer to prevent electrical interference between neighboring wave gages.

c. A Cushing Inc. Model 612-P "velmeter" converter was used in conjunction with a miniature electromagnetic cylindrical sensor (Model 600-40). These were mainly used to measure the jet velocity at several locations along the centerline of the wave tank. The sensor was 0.74 cm in diameter, with its electrodes 0.8 cm away from its tip. The minimum time constant of the "velmeter" converter is 0.1 second.

Experimental Procedures

- a. Surface wave parameters were measured without the jet being discharged. Wave measurements included the time history of the water surface elevations at several points along the wave travel. No cross waves were found to exist for the range of waves generated, so that the waves were purely two dimensional. Dye crystals were dropped into the tank, near the bottom, for flow visualization of the waves bottom mass transport, and a time sequence of color photographs was taken.
- b. A turbulent jet was also generated separately. Sufficient time was allowed to pass for steady conditions of the jet to be developed. Dye was usually inserted in the jet for flow visualization. As for the case of the waves, color photographs were taken for the growth of the dye crystals on the bottom. Velocity measurements, using electromagnetic flow meter and the hot film sensor, were made at several locations along the longitudinal axis of the jet.
- c. Data on the wave-jet flow pattern was obtained by generating the waves followed by the jet flow opposing the waves. A steady state of the flow field was usually reached within a few minutes. As before, color photographs were taken for the bottom flow pattern.

Analog to Digital Conversion:

The analog outputs from the measuring devices were recorded, digitized, and then processed on a CDC 6400 computer. Tests with data samples of both the water surface elevations and instantaneous particle velocity, showed that the time series obtained in these experiments proved to be a weakly stationary ergodic random process. Choice of digitization time interval and record length requires a knowledge of the frequency range of interest for the particular parameter measured in the experiments. For water surface elevations the analog signal was digitized at a rate 10 samples per second. The time interval chosen for the velocity analog signal to be digitized was 20 samples per second. This was done as most of the energy within a spectrum lies generally within the low frequency band. It

has been found that over the range of wave frequencies generated in this study (0.8 - 1.4 Hz), approximately 100 seconds were sufficient for accurate estimate of time mean and spectral quantities.

RESULTS

Current Modifications

In this section, experimental results regarding the effect of opposing wave motion on the horizontal shear of the current ξ and on the modification of the rate of spreading of the jet are presented.

The experimental data taken along the longitudinal axis of the jet show that in the presence of waves mean velocities of the current near the bottom are decreased with a tendency of the current shear near the water surface to increase. As wave frequency and amplitude increase, the decrease of the mean velocities near the bottom becomes more prominent with an increase of the mean velocities near the water surface [Ismail, (6,8)].

The experimental data also indicate that there is a net decrease in the momentum density of the current along the jet longitudinal axis which is accompanied by an increase in the spreading rate of the jet. The increase of spreading rate of the jet was deduced experimentally using a photographic means and was compared with that derived theoretically (Eq. 8). The comparison shows that for linear waves the agreement between the theory and experiment is excellent for a distance less than $2X/W_0 \approx 64$ [Ismail (9)].

Surface Waves Modifications

Surface waves modifications due to the opposing non-uniform current are presented in the following subsections. First, the effect of the jet on the modification of wave amplitudes is presented. Second, modifications of the wave particle velocities by the current are presented, followed by modifications of the wave bottom mass transport.

Wave amplitudes

The experimental results show that waves were decreased in length and increased in height as waves propagated into the jet. Waves were also shown to be refracted as they propagated into the jet. However, the degree of refraction was slight as the dimensionless parameter G was kept large in the design of experiments in order to focus on the direct dynamical aspects of the interaction.

Figures 3 and 4 show respectively the spectrum of the wave energy potential density for three waves of different characteristics in case of waves on still water and waves in the presence of the current. The results shown on Fig. 4 show that for waves of higher Ursell number the second and higher harmonics have larger normalized energy density. The amplification of wave amplitude due to the

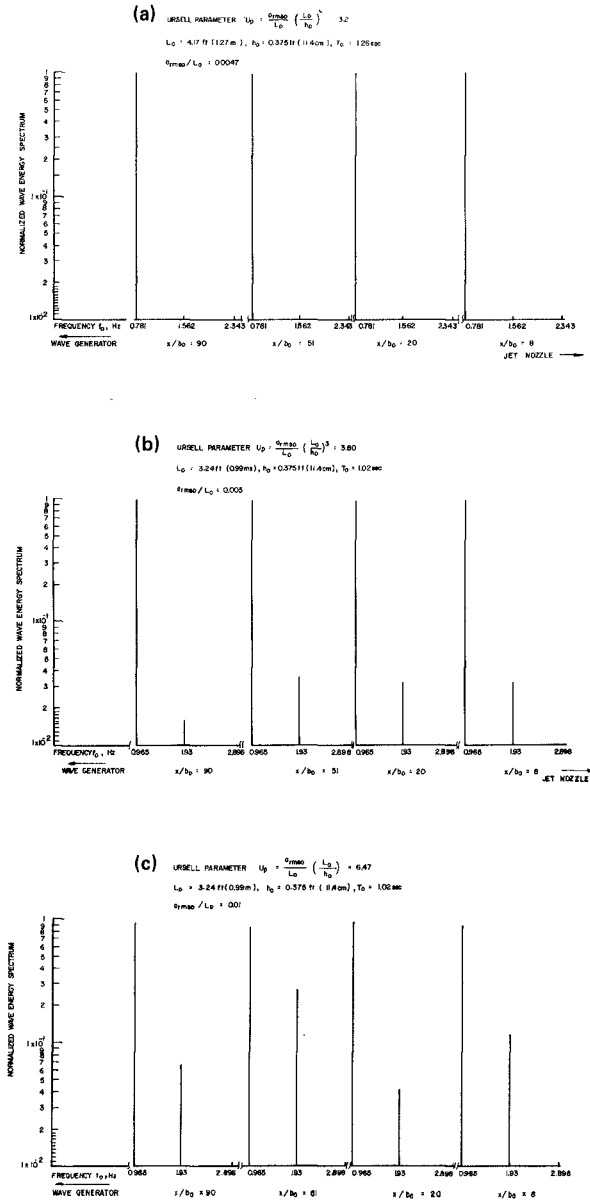


FIG. 3 Frequency Line Spectrum for Waves on Still Water (Energy Density is normalized by the Variance $\overline{\eta^2}$)